# Nonstretch NMO

*H. Perroud and M. Tygel*

**email:** *Herve.Perroud@univ-pau.fr*
**keywords:** *NMO, stretch, traveltime*

**ABSTRACT**

*We describe a new implementation of the normal-moveout (NMO) correction, that is routinely applied to common-midpoint (CMP) reflections prior stacking. The procedure, called nonstretch NMO, automatically avoids the undesirable stretch effects that are present in conventional NMO. Under nonstretch NMO, a significant range of large offsets, that would normally be muted in the case of conventional NMO, can be kept and used, leading to better stack and velocity determinations. We illustrate the use of nonstretch NMO by its application to synthetic and real datasets, obtained from high-resolution (HR) seismic and ground-penetrating radar (GPR) measurements.*

## INTRODUCTION

As shown firstly by Buchholtz (1972), conventional application of NMO correction to a CMP reflection generates a stretch which increases with offset and decreases with zero-offset time. The discussion on the effect of NMO correction on reflection data has always been a topic of interest. For our needs, we cite one of the earliest references Dunkin and Levin (1973). Due to stretch, a number of NMO-corrected traces needs to be muted after a given offset. For this purpose, an acceptable stretch limit has to be fixed by the user, and the choice of this limit could have a great impact on the frequency content of the stack images Miller (1992). As a consequence, the large-aperture traces cannot be used in velocity analysis and stacking processes. This is particularly harmful for shallow reflectors, which present relatively large offsets with respect to depth (or traveltime). It can also be a significant handicap for the search of subtle traps Noah (1996).

The proposed nonstretch NMO can be also advantageous for amplitude-versus-offset (AVO) purposes. In fact, increasing the offsets in which key reflection events (such as, e.g., top-of-reservoir reflections) do not suffer from NMO stretch, can be useful to extend AVO to a larger range, so that the estimations AVO attributes can be made more reliable. Of course, possible interference with neighboring events may limit the application of this approach.

The origin of the NMO stretch lies in the form of the hyperbolic equation

$$t^2(h) = t_0^2 + 4h^2/v_{nmo}^2, \tag{1}$$

that is used to describe the reflection time $t$ as a function of half-offset, $h$. Here, $t_0$ stands for the zero-offset (ZO) traveltime and $v_{nmo}$ represents the NMO velocity, which is an estimation of the root-mean-square (RMS) velocity in the case of flat-layered media. From simple geometrical considerations, it can be verified that equation (1) represents a hyperbola whose asymptote passes through the origin and has slope equal to $2v_{nmo}^{-1}$. For a band-limited source pulse, the reflection event of traveltime (1) is generally observed as a strip of constant width (the pulse width) around that curve. The ideal NMO correction should be the one that would simply move the whole strip around the traveltime curve (1) onto a corresponding strip (of the same width) around the horizontal line $t = t_0$.

For a user-selected value of $t_0$, an estimation of $v_{nmo}$ is conducted as a one-parameter search that maximizes the coherency (semblance) of the data within the CMP gather. The procedure is usually called NMO

velocity analysis, or velocity scan. After an acceptable estimate of $v_{nmo}$ is obtained, conventional NMO correction transforms samples $t(h)+\tau$ in the vicinity of the traveltime curve (1) onto their corresponding values $t_0+\tau'$ according to the equation

$$(t_0+\tau')^2 = (t(h)+\tau)^2 - 4h^2/v_{nmo}^2. \tag{2}$$

Comparison of equations (1) and (2) yields the well-known first-order relationship $\tau'/\tau = t(h)/t_0$ Dunkin and Levin (1973), which defines the stretch ratio. To understand why the conventional NMO correction, as provided by equation (2), introduces a stretch in the output signal, we refer to (Figure 1, left). There we see that, for fixed $v_{nmo}$, the NMO traveltime curves for zero-offset times $t_0$ and $t_0+\tau$ are both converging, for large offsets, towards their common asymptote $t = 2h.v_{nmo}^{-1}$. This means that these hyperbolae are not parallel to each other: after moveout, the shape of the reflection pulse will therefore be stretched since, within the same trace, smaller time samples will experience a larger moveout than larger time samples. As seen from the above analysis, one approach to avoid the NMO stretch, is to introduce a different traveltime moveout expression that keeps as much as possible the parallelism between the hyperbolae when changing zero-offset time. This idea was proposed by de Bazelaire (1988) with the so-called method of shifted hyperbolae. In this formulation, the scanned parameter is the focussing time of the hyperbola, $t_p$, instead of the velocity $v_{nmo}$. Another approach was introduced as the block-move-sum (BMS) concept Rupert and Chun (1975), which applies a series of static shifts to blocks of data, followed by a summation. BMS has been the subject of further developments, as recently illustrated by Brower (2002), where an up-to-date references list can be found. In the present paper, however, we want to stay as close as possible to the widely used NMO method and traveltime equation (1), so that *a quasi-static NMO shift can be obtained from the usual dynamic NMO process, in a manner similar to a block moveout process. In this way,* our new approach can be adopted by the users of the traditional NMO without a severe change of processing tools and habits.

It is to be remarked that the formulation and analysis of the NMO stretch phenomenon presented in this work is very similar to the one recently described in Mann and Höcht (2002). The main point is that, in order to avoid stretch, the NMO-velocity has to be corrected both in zero-offset time shift and offset. The NMO stretch elimination procedure proposed and implemented here, considers the full, offset-dependent NMO-velocity correction, as opposed to Mann and Höcht (2002) that employs an offset-independent approximation of that correction.

## NONSTRETCH NMO: THEORY

As stated above, to avoid stretch, one has to keep parallelism of NMO traveltimes as much as possible. However, strict (global) parallelism is not achievable using the classical NMO equation (1), since their asymptotes intersect at the origin. So the problem can be formulated in the following manner: what condition should we impose such that the NMO for a single trace can be performed without stretch? The only parameter that has some degree of freedom is the $v_{nmo}$, which is also related to the slope of the asymptote. Nonstretch NMO, therefore, proposes to adjust it so that local parallelism can be obtained. To explain how this can be done, we refer to (Figure 1, right) and consider the equation

$$(t(h)+\tau)^2 = (t_0+\tau)^2 + 4h^2/v^2(\tau). \tag{3}$$

Here, $\tau$ is a time shift and $v(\tau)$ is the adjusted velocity that eliminates the stretch for that half-offset $h$. Note that equation (3) is the same as equation (2), with the exception that the adjusted velocity, $v(\tau)$, replaces the fixed NMO-velocity, $v_{nmo}$, and the non-stretch condition, $\tau' = \tau$, has been imposed. After simple manipulations combining equations (1) and (3), we obtain the important expression

$$v(\tau) = v_{nmo}\left(1+\frac{2\tau}{t(h)+t_0}\right)^{-1/2}, \tag{4}$$

that determines the adjusted velocity $v(\tau)$ for a reflection event, characterized by $t_0$ and $v_{nmo}$, at offset $h$ and time shift $\tau$. To better reveal the physical meaning of equation (4), it is useful to recast it in the form

$$v(\tau) = v_{nmo}\left(1+\frac{2}{1+\sqrt{1+a^2}}\frac{\tau}{t_0}\right)^{-1/2}, \quad \text{with } a = \frac{2h}{t_0.v_{nmo}}. \tag{5}$$

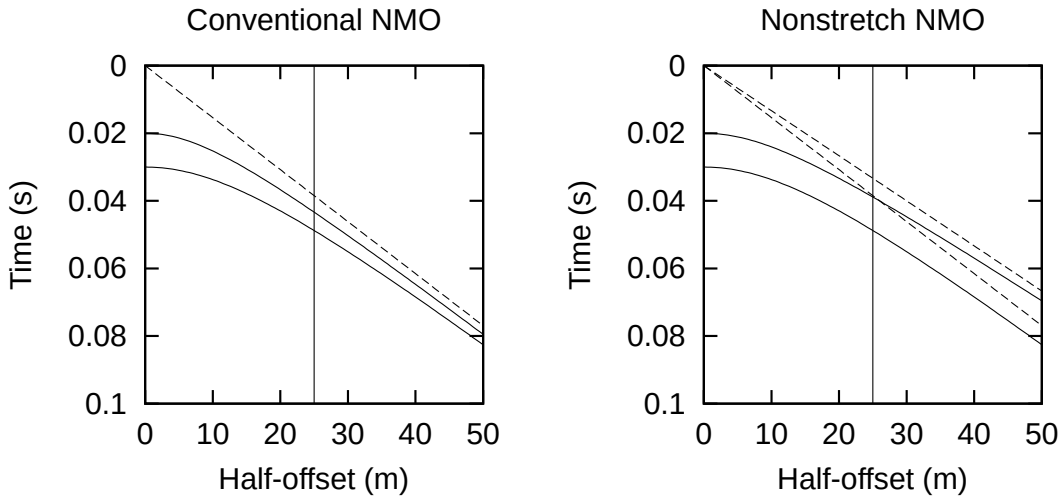


**Figure 1:** Comparison between conventional NMO (left) and nonstretch NMO (right). The hyperbolae corresponding to the onset and the end of a reflection event are shown (solid lines), together with their asymptotes (dashed lines). At half-offset $h$ equal 25 m, the vertical line reveals the separation between the hyperbolae. For conventional NMO, the hyperbolae converge with $h$, while for nonstretch NMO, their distance is kept equal for the chosen $h$.

We call the quantity $a = 2h/t_0 v_{nmo}$ the *geometrical aperture* in the effective constant-velocity medium defined by $t_0$ and $v_{nmo}$. Under the usual assumption of a model that consists of flat homogeneous layers, the geometrical aperture $a$ is simply the tangent of the incidence angle onto an effective reflector at depth $v_{nmo}t_0/2$ for a source-receiver pair with half-offset $h$. In such a media, the NMO stretch factor is linked to the aperture $a$ by the formula $\tau'/\tau = t(h)/t_0 = \sqrt{1+a^2}$. This makes explicit the relationship between the NMO stretch and the nonstretch NMO adjusted velocity. We see that the required NMO-velocity correction depends both on time-shift and offset. Except for a change in notation, equation (5) coincides with its counterpart equation (4) in Mann and Höcht (2002).

Equation (5) better displays the main factors that influence the determination of $v(\tau)$, namely the zero-offset time of the event $t_0$ and the geometrical aperture $a$. For a given event, the strongest effect onto the stacking velocity corresponds to null aperture ($a = 0$), where equation (5) reduces to

$$v(\tau) = v_{nmo}\left(1 + \frac{\tau}{t_0}\right)^{-1/2} \tag{6}$$

It corresponds to maintain constant the product $(t_0 + \tau)v(\tau)^2$, and thus the curvature of the hyperbolic traveltime curves at null offset. On the other hand, if the aperture $a$ gets very large, equation (5) tends to its limiting value $v(\tau) = v_{nmo}$, which means that $v_{nmo}$ has to be kept constant over the whole pulse length. For the intermediate, more usual, apertures, the adjusted velocity lies between these two extreme cases. Moreover, it can be seen from equation (4) that, for the set of events recorded on a given trace, stronger effects onto the stacking velocity are observed at shorter zero-offset times. Equation (6), that can be interpreted as an offset-independent approximation of the NMO-velocity to avoid stretch, is the one selected in Mann and Höcht (2002).

From equation (4), as $t(h)$ and $t_0$ are strictly positive, we see that $v(\tau)$ always decreases when the time shift $\tau$ increases. Therefore, even setting NMO velocity constant is not sufficient to avoid stretch, as done in the constant-velocity-stack (CVS) approach. In addition, the classical increase of NMO velocity with time that results from interpolating the time-velocity distribution is going the wrong way and further increases the stretch effect of the NMO.

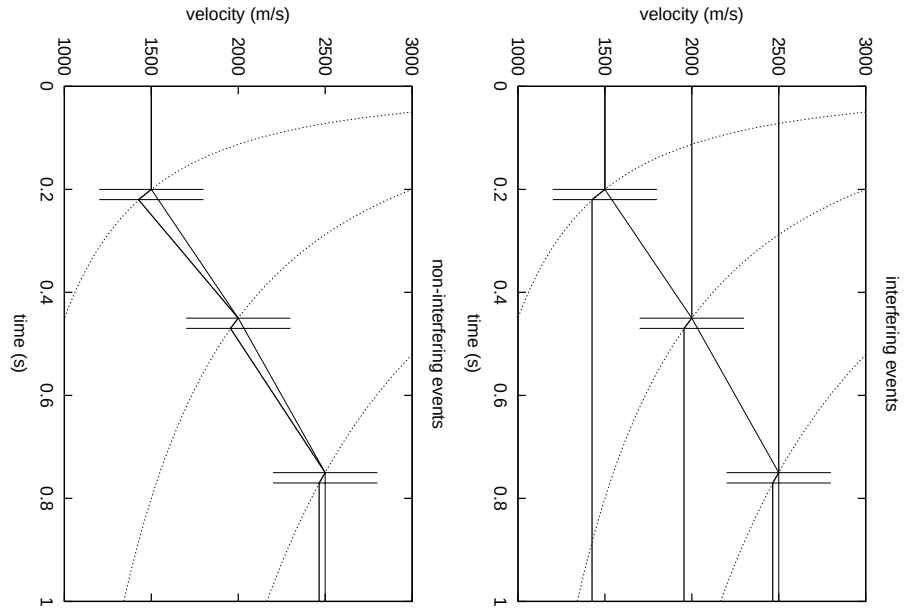


**Figure 2:** Construction of velocity distribution in the case of non-interfering (left) or interfering (right) events. Thick solid lines represent the modified velocity distributions that replace the corresponding conventional ones, shown as thin solid lines. Dotted lines represent the velocity functions derived from equation (4) for individually picked events, computed for half-offset $h$ equal 200 m. They are used only in the time-range that refers to the pulse length between two horizontal bars.

## NONSTRETCH NMO: IMPLEMENTATION

Based on the above considerations, we propose the following scheme to implement the nonstretch NMO. After performing the usual NMO velocity analysis, which estimates $t_0$ and $v_{nmo}$ for each reflection event, a specific velocity distribution is constructed for each trace in the following manner: for each event, the originally picked time-velocity point is replaced by a curve segment which follows equation (4) (see Figure 2, left). Note that the only quantity that is additionally needed is the range for argument $\tau$. A good estimation of this range can be obtained as the inverse of the bandwidth of the propagating signal. In this way, the whole procedure can be made automatically. Obviously, the trace-dependent, time-velocity distribution obtained here is solely used for applying the nonstretch NMO correction and should be discarded after this purpose. As the non-stretch condition implies that the velocity decreases with time in the $\tau$-range, it means that the interpolated NMO velocity between events will grow more rapidly, and thus the NMO stretch effect will be increased between events. It is therefore necessary not to forget any reflection event in the velocity picking, so that the increased stretch will concern only the noise between events.

The classical NMO processing tools usually provide an upper limit to acceptable stretch, the stretch-mute ratio, all samples with a NMO stretch exceeding this ratio being simply muted. This mute renders impossible an exact inverse NMO process, opposite to the case of nonstretch NMO. This new process can therefore be quite helpful for any processing chain in which NMO can be temporarily applied, and later removed.

However, for the large apertures encountered in near surface seismics or GPR studies, NMO stretch leads to a very severe mute of superficial events. This results on a blind zone at the top of the sections. On the other hand, the stretch-mute ratio provides a way to limit the offset used in the CMP gather analysis and stack, and therefore acts as an implicit trace filter. When applying the proposed nonstretch NMO, new problems are bound to arise with long offsets, as for example interferences between crossing events. As shown in the examples below, a way to circumvent these situations is to process the reflection events one at a time. To do so, we construct the hyperbolae corresponding to the onset of each event from the

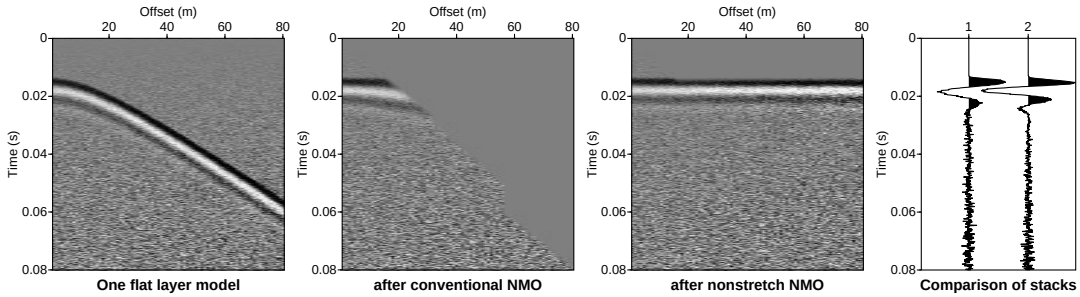


**Figure 3:** Comparison between conventional NMO and nonstretch NMO for a single flat layer model. In the comparison of stacks, the left traces were obtained by conventional NMO, whereas the right ones were obtained by nonstretch NMO. The synthetic data has been obtained by ray tracing followed by wavelet convolution and noise addition. Amplitudes are not realistic. However, geometrical spreading is included and was compensated in the processing.

time-velocity distribution obtained by the NMO velocity scan. Then, for each event, we mute all samples above the corresponding hyperbola and below those for the next events and apply the nonstretch NMO. As each event is processed individually, the modified velocity distribution needs not to be interpolated between events. It is simply extrapolated to the full time range (see Figure 2, right). As a consequence, this limits the stretch induced by NMO *between* events. Furthermore, note that the NMO velocity above the event is the largest, and the one below the event is the smallest. As a consequence, there can be no fit between that event and the NMO stacking curves apart from those that refer to zero-offset traveltimes $t_0$ that belong to the very time range for that event. This approach is a natural solution to the crossing event problem (even if a part of the event is muted). A complete processed trace is later recovered by summing the contributions from all events. Note that since each event does not suffer from NMO stretch mute, inverse NMO should still be possible.

### Application to synthetic datasets

We have tested the nonstretch NMO process in four different cases. For the first two, we used synthetic datasets where the exact zero-offset times and RMS velocities are known. In the first example, we were interested only in the kinematics. The dataset was obtained by ray tracing, in a model with only one flat layer, presenting a very large aperture (maximum half-offset of 40 m for a reflector depth of 10 m). The results of both conventional and nonstretch NMO are shown in Figure 3. In both cases, the exact $t_0$ and $v_{nmo}$ were used, and the stretch-mute ratio was fixed at 1.3. The stacked traces shown on the right permit to evaluate the improvement provided by nonstretch NMO. Right traces, corresponding to nonstretch NMO, reveal a sharper and cleaner recovered pulse, than the one in left traces, corresponding to conventional NMO. This indicates that the new process is expected to yield a better detection and a better resolution, although this should be verified with true-amplitude data. The second example was obtained by an acoustic finite-differences simulation in a flat multi-layer model. It presents, therefore, more realistic amplitudes. The maximum aperture corresponding to the different reflectors varies from 0.5 to 4. The reflection data are interfering with direct waves and multiples. Furthermore the two top events are interfering with each other. To simulate the effect of ground-roll in near-surface land data, a mute was applied to eliminate the part of the section usually covered by surface waves. The results of both conventional and nonstretch NMO are shown in Figure 4, together with the corresponding stacked traces. Once again, the improvement brought by nonstretch NMO is very striking in the upper part of the trace. Due to low aperture, the lower part of the trace stays unchanged.

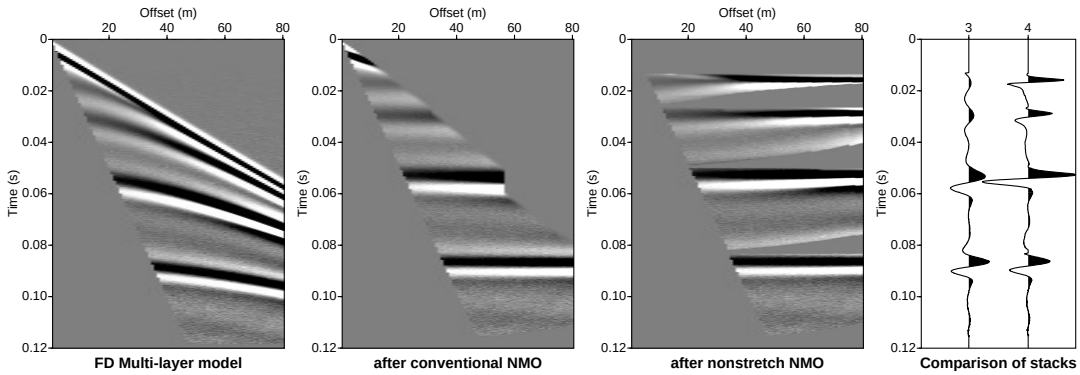


**Figure 4:** Comparison of conventional NMO and nonstretch NMO for a flat multi-layered model. In the comparison of stacks, the left traces were obtained by conventional NMO, whereas the right ones were obtained by nonstretch NMO. The synthetic data has been obtained by acoustic finite-differences simulation and noise addition.

### Application to a seismic real datset

As a third example, we considered a high-resolution (HR) seismic real dataset, obtained from measurements using a high-frequency mini-sosie-type source from Vibrometrics. A typical CMP is shown in Figure 5. It reveals a set of hyperbolic events corresponding to times between 0.01 and 0.06 s, that is roughly between 5 and 30 m depth. For the shown offset range, the aperture varies from more than 3 at the top, to less than 1 at the bottom. It is to be noted that the first event has been interpreted as a refraction arrival, and, as a consequence, not picked.

Applied with the usual stretch mute ratio of 1.3, conventional NMO, completely fails to image the first event. Moreover, the second event can only be marginally imaged, due to the intense stretch and mute. On the contrary, nonstretch NMO is able to align the reflected signals over the whole offset range, providing a much better criterion for the choice of NMO velocities. In addition, the recovered pulse shape after nonstrecth NMO seems more regular, so that further signal processing is expected to be more accurate and efficient.

Figure 6 shows the semblance map that is used for velocity picking, together with the picked and adjusted velocity laws that result from conventional NMO (left) and nonstretch NMO (right), respectively. We can readily see, especially for upper events, that semblance maxima present a clear elongation towards smaller velocity and larger time. This behavior poses a challenge to the interpreter, in particular with closely-separated events. Observe that the adjusted velocities after nonstretch NMO naturally fit that tendency, in the same way as an automatic picking of semblance maxima would do. The characteristic display of adjusted velocities in nonstretch NMO, which can be of great help for the interpreter in the velocity picking phase, can be considered as another clear advantage over conventional NMO, or even block moveout techniques.

### Application to a GPR real dataset

Our final test was carried out on a real GPR multi-offset dataset, with offsets ranging from 0.6 m to 6 m, 28 fold, and penetration depth of about 5 m. The uppermost event corresponds to a maximum aperture of about 4, while it is less than 1 for the lowermost one. The results of both conventional (stretch-mute ratio 1.3) and nonstretch NMO on a single CMP gather are shown in Figure 7. Crossing events can be observed for large offsets. These were muted by conventional NMO, but correctly recovered by nonstretch NMO. It is to be noticed how different the stacked traces are in their uppermost part. This emphasizes the interest of this new process. In particular, one can observe that the event at time 0.05 ms has completely disappeared after conventional NMO, due to its phase shift with offset.

To check the potential of nonstretch NMO to improve the time images, it has been applied to all CMP

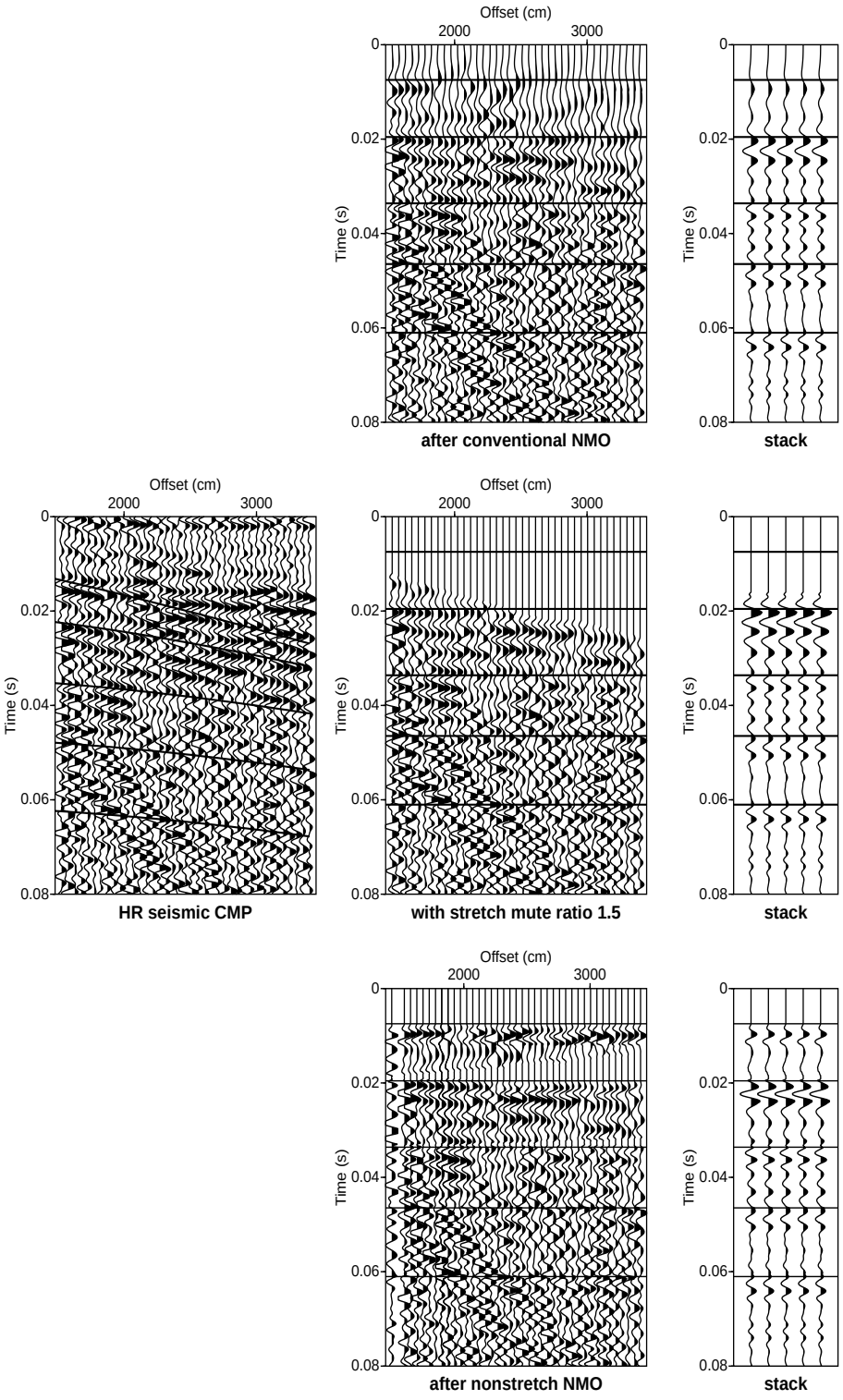


**Figure 5:** Comparison between conventional NMO and nonstretch NMO for a HR seismic example. In the comparison of stacks, the left traces were obtained by conventional NMO, whereas the right ones were obtained by nonstretch NMO.

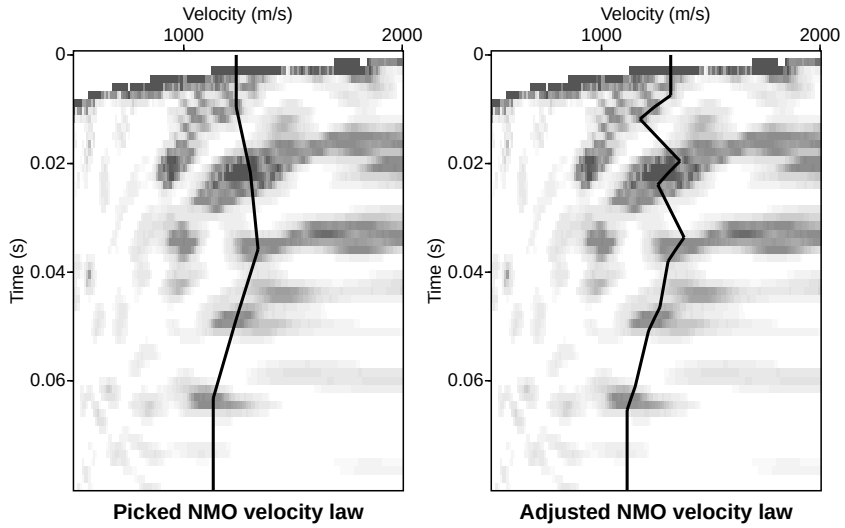


**Figure 6:** Comparison between picked and adjusted velocity laws in conventional NMO and nonstretch NMO for the HR seismic example. It can be seen how the second fits the shape of the semblance maxima, shown as the background image.

gathers, spaced every 0.1 m along the 55 m of the GPR profile. Velocities were picked using a conventional semblance map, but were adjusted to best flatten the reflection events after nonstretch NMO, rather than conventional NMO. From these picked velocities, both conventional (stretch-mute ratio 1.5) and nonstretch NMO were applied. The resulting stack sections, after amplitude balancing, are displayed in Figure 8. Although the two sections bear strong resemblance, significant differences can still be observed. Firstly, the upper half of the stack section obtained with nonstretch NMO reveals, as expected, more focussed events, and a much clearer rendering of the channel filling in its right part. This is particularly significant since that part of the section has a lower signal-to-noise ratio, and therefore needs a larger number of traces to define a clear image. This is exactly what our new process provides. Second, all over the section, nonstretch NMO generates less smoothed images. As a matter of fact, conventional NMO section appears to be a smoothed version of its nonstretch NMO counterpart. It is interesting to note that the NMO stretch effect, which induces a dilution of the vertical resolution, also seems to generate a bit of horizontal smoothing.

To quantitatively evaluate the improvement on seismic resolution brought by nonstretch NMO, we performed a spectral analysis of both stack sections of Figure 8. The obtained average amplitude spectra are shown in Figure 9. As the NMO stretch effect varies with time, the analysis was carried out on two time gates of equal duration, 0.06 microsecond, starting just below the top mute. The limit between these time-gates corresponds to a geometrical aperture around 1. Peak frequencies and frequency bandwidths estimated from these spectra, revealed that the greater change is obtained in the upper part of the sections. In that region, peak frequency increased from 102 Mhz to 119 Mhz, and bandwidth from 94 Mhz to 105 Mhz. In the lower part of the sections, no significant change can be noticed, apart from a slight increase (from 114 to 117 Mhz) of the peak frequency. As expected, nonstretch NMO appears to be most efficient when the seismic aperture is larger. In this way, it should be most helpful in near-surface geophysics, e.g. in HR seismics or GPR studies.

## CONCLUSIONS

We presented a new method, called nonstretch NMO, that adapts the conventional NMO procedure with the aim of producing corrected traces with no stretch effects. In this way, the proposed method can be easily incorporated to the routine processing sequences, say in seismics or GPR investigations. To illustrate the method, we applied the procedure to simple synthetic data as well as to real data examples. In all cases,

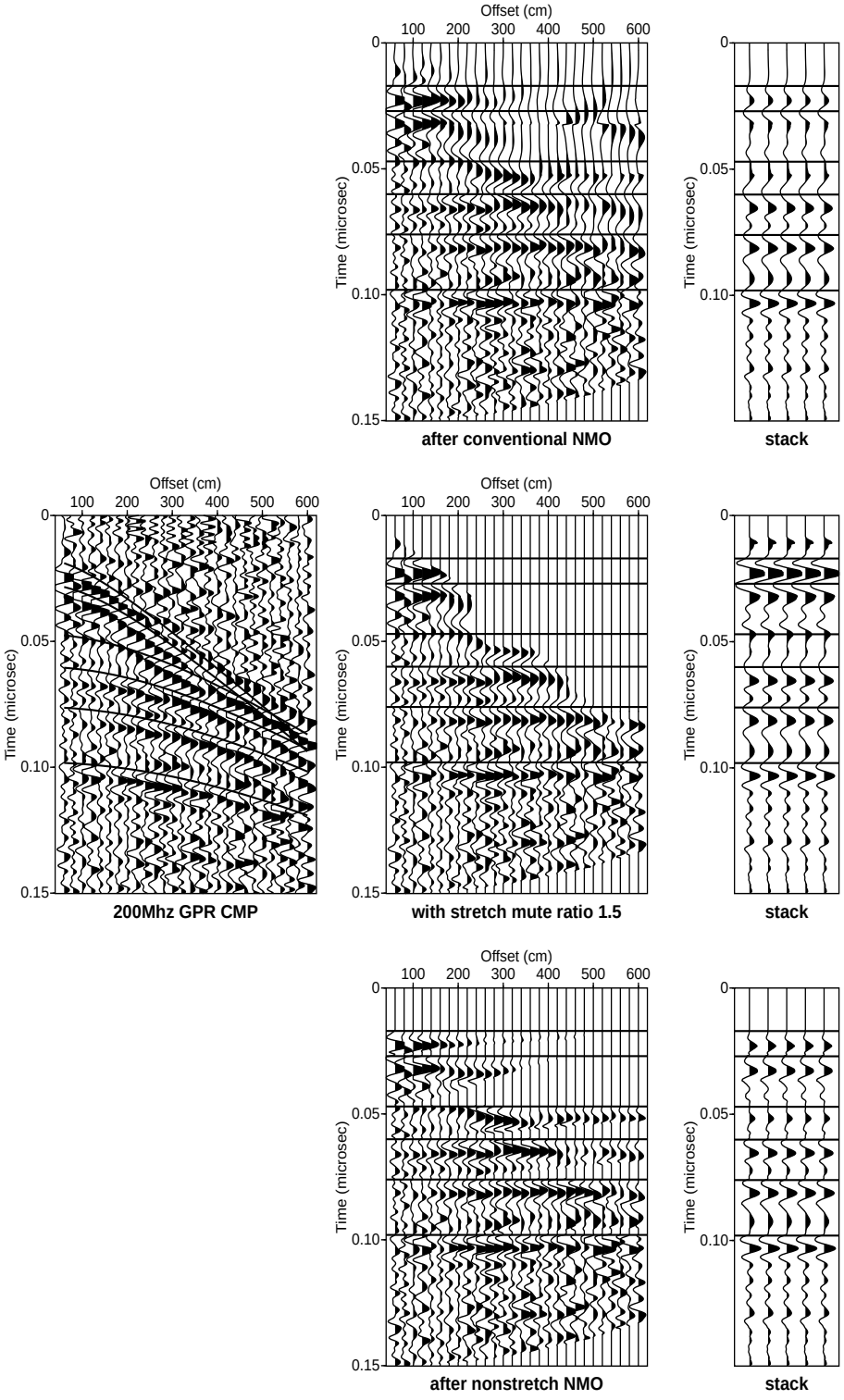


**Figure 7:** Comparison between conventional NMO and nonstretch NMO for a real GPR CMP gather. In the comparison of stacks, the left traces were obtained by conventional NMO, whereas the right ones were obtained by nonstretch NMO.

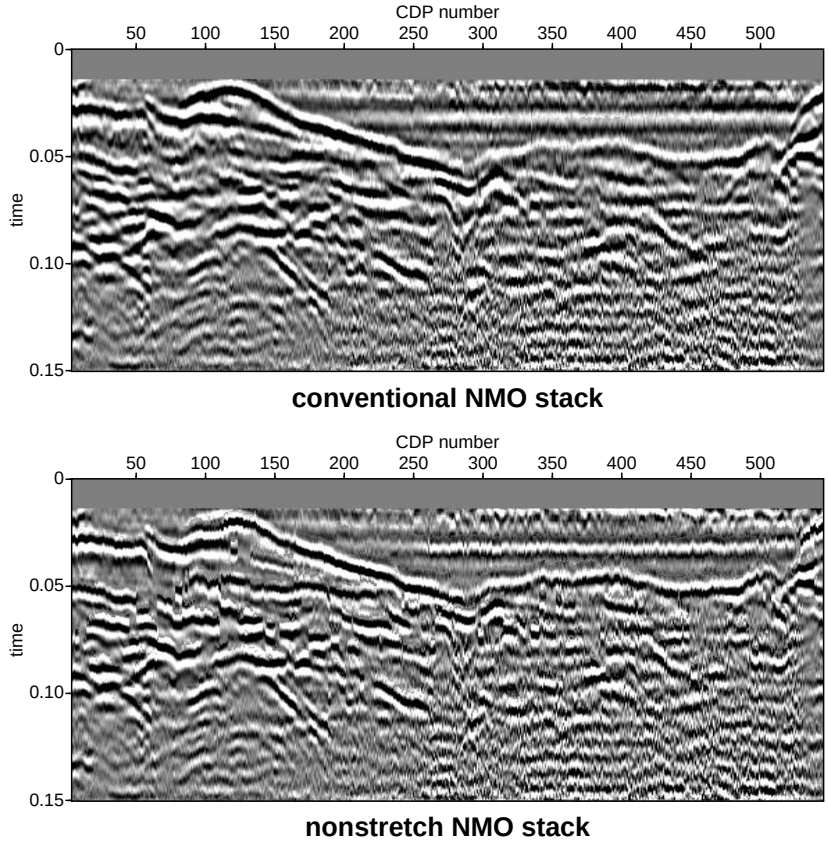


**Figure 8:** Comparison between conventional NMO and nonstretch NMO for a complete stack section. Trace amplitudes were balanced to better represent the kinematic aspects of the GPR images.

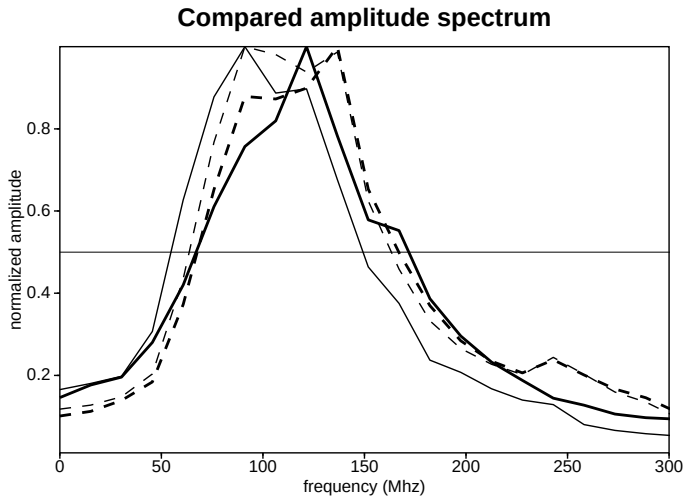


**Figure 9:** Comparison of amplitude spectrum for conventional NMO and nonstretch NMO stack sections. Thick (resp. thin) solid lines represent the average amplitude spectrum for the upper part of the nonstretch (resp. conventional) NMO stack section. Dashed lines represent the same for the lower part of the stack sections.

the new method was able to significantly enlarge the offset range of the undistorted NMO corrected traces and thus improve the quality and resolution of the time images. It appears particularly useful when the geometrical aperture exceeds 1, e.g. when half-offset is larger than reflector depth. Also a number of remarks concerning the implementation have been made. This includes in particular the difficult case of crossing events. We finally note that the proposed nonstretch NMO may be also beneficial for amplitude-versus-offset (AVO) analysis, since, away from interfering events, larger, undistorted, offsets will be available for attribute inversion.

## ACKNOWLEDGMENTS

We like to thank the Research Foundation of the State of São Paulo (FAPESP, Brazil), for financial support (Grant 01/01068-0) and the stay of H.P. at Unicamp, Campinas (Grant 02/06590-0). The idea to use the inverse of the signal bandwidth in the nonstretch NMO process was suggested by E. de Bazelaire. The finite-differences code used is maintained by D. Rousset. The GPR data were acquired and processed with the help of P. Senechal. All NMO and velocity scan procedures have been conducted with the Seismic Unix software, release 35.3, Center for Wave Phenomena, Colorado School of Mines. We finally thank the support of the sponsors of the *Wave Inversion Technology (WIT) Consortium*.

## REFERENCES

Brower, J. H. (2002). Improved nmo correction with a specific application to shallow seismic data. *Geophys. Prosp.*, 50:225–237.

Buchholtz, H. (1972). A note on signal distortion due to dynamic (nmo) corrections. *Geophys. Prosp.*, 20(02):395–402.

de Bazelaire, E. (1988). Normal moveout revisited - Inhomogeneous media and curved interfaces. *Geophysics*, 53(02):143–157.

Dunkin, J. W. and Levin, F. K. (1973). Effect of normal moveout on a seismic pulse. *Geophysics*, 38(04):635–642.

Mann, J. and Höcht, G. (2002). Short note: The pulse stretch phenomenon in the context of data-driven imaging methods. *Wave Inversion Technology (WIT) Report*, 6:35–40.

Miller, R. D. (1992). Normal moveout stretch mute on shallow-reflection data. *Geophysics*, 57(11):1502–1507.

Noah, J. T. (1996). Interpreter's corner - NMO stretch and subtle traps. *The Leading Edge*, 15(05):345–347. Discussion in TLE-15-9-990.

Rupert, G. B. and Chun, J. H. (1975). The block move sum normal moveout correction. *Geophysics*, 40(01):17–24.